IOP Conf. Series: Materials Science and Engineering **324** (2018) 012075 doi:10.1088/1757-899X/324/1/012075

The Cross-Sectional Investigation of Oxide Scale FeCr Alloys and Commercial Ferritic Steel Implanted with Lanthanum and Titanium Dopants after Oxidation Test at 900^{O}C

Darwin Sebayang[1], Hendi Saryanto[1, 2], Pudji Untoro[3], Tjipto Sujitno[4]

[1]Mercu Buana University, Jln. Meruya Selatan, Jakarta Barat, Indonesia
[2]Garuda Muda Institute, Jakarta, Indonesia
[3]Surya University, Jln. Boulevard Gading Serpong, Banten-Indonesia
[4]Centre For Accelerator and Material Process Technology. BATAN JL. Babarsari, D.I Yogayakarta, 55281, Indonesia

Email: hsaryanto@gmail.com & d_sebayang@hotmail.com

Abstract. The cross-sectional examinations of oxide scales formed by oxidation on the surface of FeCr alloys and Ferritic Steel that implanted with lanthanum and titanium dopants were observed and investigated. Scanning electron microscopy (SEM) coupled with energy dispersive X-ray spectroscopy (EDS) has been used to study the cross-sectional oxides produced by specimens after oxidation process. X-ray diffraction (XRD) analysis was used to strengthen the analysis of the oxide scale morphology, oxide phases and oxidation products. Cross-sectional observations show the effectiveness of La implantation for improving thinner and stronger scale/substrate interface during oxidation process. The result shows that the thickness of oxide scales formed on the surface of La implanted FeCr alloy and ferritic steel was found less than 3 μm and 300 μm, respectively. The oxide scale formed on the surface of La implanted specimens consisted roughly of Cr_2O_3 with a small amount of FeO mixture. The oxidation resistance of FeCr alloy that implanted with Lanthanum showed better quality than that of commercial alloy. The beneficial effect of La implanted sample on the oxidation resistance was clearly visible to improve the adherence of oxide scale. Cross-sectional observations revealed the effectiveness of La implantation for improving thinner and stronger scale/substrate interface during oxidation process which presents the homogenous structure with good adherence and a uniform inter-diffusion layer between substrate and oxide layer.

Keywords: Cr_2O_3, FeCr Alloys, Ferritic Steel, Crystallite Size, Lanthanum, Titanium

1. Introduction

The main problem with the use of conventional steel alloy is their inadequate high-temperature oxidation resistance [1]. Under SOFC operating conditions, ferritic steel form the oxide scale that is susceptible to spalling during normal fuel cell operation, in particular during thermal cycling encountered at start-up and shut down [2]. The extensive oxide losses from the surface or oxide spalling usually occur, which has become a serious challenge that leads to serious deterioration of the cell performances [3, 15]. Therefore, the alloys stabilization and oxidation performances at the high temperatures are essential to

enhanced performance of the cell, chromium evaporation is known to be a major problem in SOFC stacks since volatile chromium is gets deposited on the cathode and poisons the oxygen electrode [4]. To enable practical application, two classes of technology can be approached to reduce the growth rate of the oxide scale, the first is to develop nanostructured alloys, and the other is to conduct surface treatment of the developed or available alloy with a reactive element [5,15]. FeCr alloys and ferritic stainless steels exhibit excellent properties as interconnect material in SOFCs [6]. The oxidation performance of FeCr used in high-temperature applications (such as Interconnector in SOFC) depends on their potential to form and maintain a Cr-rich protective oxide scale [7-8]. Technical requirements to be used as interconnect in SOFC should fulfill a number of specific requirements, i.e. a high oxidation resistance, a high electrical conductivity of the surface oxide scales, gas tightness, and a coefficient of thermal expansion matched to the electrolyte and the electrodes [9-10]. The role of the interconnect component in SOFC units is to electrically connect individual cells in series to form a multi-cell stack with higher power density. FeCr and Ferritic stainless steels have many desirable properties for use in solid oxide cell stacks and are the most common type of materials used as interconnect. When Cr based alloys and high-Cr ferritic steels are exposed to an oxidizing environment at elevated temperatures, an oxide layer is formed on the surface, acting as a barrier between the metal and the gas. Chromium increases the oxidation resistance of stainless steels by the formation of a chromia (Cr_2O_3) scale on the surface. Other oxides which are often encountered in the layers are iron oxides (wüstite FeO, magnetite Fe_3O_4, or hematite Fe_2O_3) [8,11-12].

Refer to our previous study [8,13-14] the cross-sectional investigation of FeCr alloy with smallest crystallite sizes can significantly reduces the growth of oxide scale and improve the high-temperature oxidation and corrosion resistance of FeCr alloy that oxidized at 900^{o}C, However, the research did not investigate the characterization of oxide scale on a cross-sectional analysis and the growth mechanism of the oxide scale of implanted specimens. Therefore, the objective of this study is to investigate the cross-sectional characterization of oxide scale formed on the surfaces of implanted specimens compare with un-implanted specimens oxidized at 900^{o}C. Oxidation kinetics, and as well as the evolution of oxide scale composition and microstructure are systematically studied. The mechanism of the formation of oxide scale on both of steels is discussed.

2. Specimens and Experimental Procedure

2.1 Specimens

The selected FeCr alloy with smallest crystallite size (38.51 nm) as the best oxidation results in our previous study [8] were selected and implanted with lanthanum and titanium dopants. Implantation of lanthanum and titanium dopants with nominal doses10^{17} ions/cm^2 was undertaken using 100 keV ion beam energy and 200 keV acceleration potential and the beam current density was maintained at 10 μA/cm^2. The depth concentration profiles of lanthanum and titanium dopants in to substrate of both type specimens were collective in Table. 1 [13-15].

Table 1. The depth concentration profiles of lanthanum and titanium dopants in to substrate of steels

Sample	Depth profile (Å)	
	Implanted with lanthanum	**Implanted with titanium**
FeCr alloys	297	706
Commercial FS	296	639

2.2. Oxidation Test

The samples of oxidation test were cut from the specimens to the size of 4x5x3 mm. The samples were subjected to oxidation tests in laboratory air at atmospheric pressure in a PROTHERM box furnace at 900^{o}C for 100 h in laboratory air at the atmospheric pressure.

2.3. Preparation of cross-section specimens

Cross-section samples are mounted using “cold-mounting” resins. Samples were placed on a commercial sample holder (cylindrical), fixed through a drop of wax. Resin (plus hardener and

accelerant) is then poured in the sample. After the sample and resin becoming a hard block, the samples were polished on the cross-sectional face up to 1500 grade SiC paper and final polishing using 0.05 µm diamond paste.

2.4. Microstructure Characterization

The oxidized alloys were investigated by a BRUKER D8 Advance X-ray diffraction (XRD) equipped with CuKα radiation and phase identification as referred to the ICDD PDF-2 database. The surface and cross-sectional morphology analyses of oxidized specimens were carried out with a JEOL JSM-6380 scanning electronic microscope (SEM) equipped with an energy-dispersive X-ray spectroscopy (EDS) analyzer. Furthermore, the best selected of oxidized specimens were analyses more detail using EDS line/mapping analysis.

3. Results and Discussion

3.1. Previous Results

The previous results on developed of FeCr Alloys, oxidation test, and parabolic rate were collected in Table 2 and Fig.1 [7, 8, 9, 10 & 11], where the parabolic rate constant (k_p) is determined by the mass gain (ΔW) per unit surface area of a specimen (A) and exposure time (t) [10, 13-15].

$$(\Delta W/A)^2 = k_p t \quad (1)$$

Table 2. Mass gain change and parabolic rate constant (k_p) of FeCr alloys after oxidized at 900°C

Specimens	Crystallite size (nm)	Mass Gain (mg/cm^2)	Parabolic Rate, k_p (mg^2/cm^4)
FeCr "A"	53.33	21.81	6.191
FeCr "B"	38.51	7.72	0.794
FeCr "C"	76.60	35.18	13.58

Table 1 show the mass gain curves of the studied alloys with different crystallite size oxidized at 900°C. Mass gain change (mg/cm^2) and parabolic rate (mg^2/cm^4) indicate that FeCr "B" as the smallest crystallite size was found as the lowest mass gain change and parabolic rate, which indicates as the best oxidation resistance.

3.2. Results of the current study

SEM morphologies of the cross-section of the oxide scale on the surface of implanted and the selected of un-implanted (FeCr "B") alloys after oxidized at 900°C for 100 h in air atmosphere are presented in Fig 1 below.

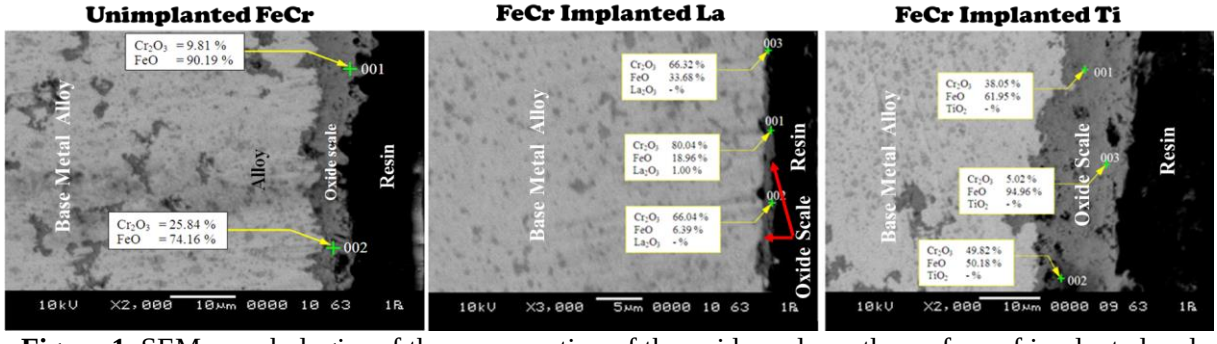

Figure 1. SEM morphologies of the cross-section of the oxide scale on the surface of implanted and un-implanted FeCr alloys oxidized at 900°C

Fig. 1 shows the cross-sectional morphology of oxide scale on the surface of implanted and un-implanted specimens oxidized at 900°C. A very thin oxide scale, less than 3 µm, had formed on the surface of FeCr alloy that implanted with lanthanum. While, the thickness of the oxide scale formed on the surface of

un-implanted FeCr alloy and FeCr alloy that implanted with titanium was formed about 8 and 15 μm, respectively. According to EDX analysis, it can be seen that the oxide scale on the surface of FeCr alloy implanted with lanthanum was dominated by the presence of Cr_2O_3 about 60.05-80.04 %, which indicates that lanthanum implantation can protect the Cr_2O_3 layer, reduce the rate of Cr evaporation and reduce the growth of the oxide scale as evidenced by the thin layer of oxide scale. However, the oxide scale formed on the surface FeCr alloy that implanted with titanium dopant indicated covered and distributed evenly with the main composition of FeO approximately 50.18-94.96%. It can be noticed that titanium implantation ineffectively promotes Cr rich oxide. At the same time, the amount of Fe increased and diffused outwards, which caused the formation and rapid growth of FeO. Furthermore, Cr_2O_3 as the protective layer becomes non-protective, due to the formation of volatile Cr_2O_3 upon exposure to oxidizing atmospheres for extended periods.

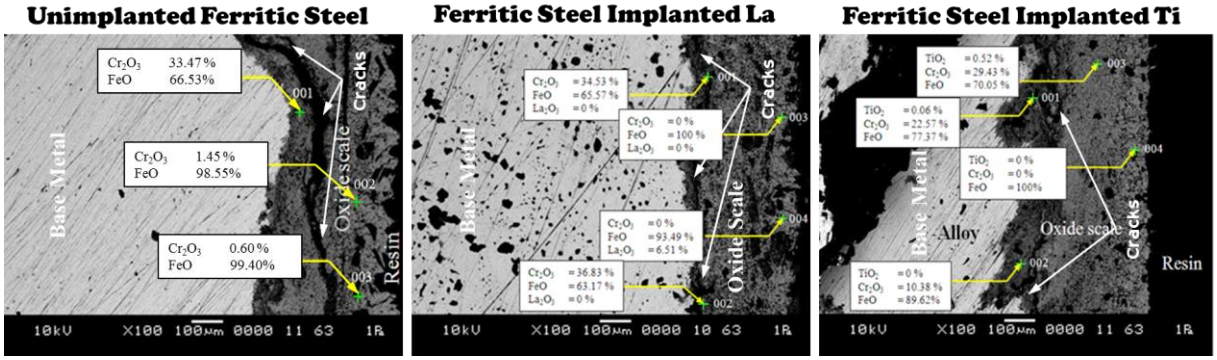

Figure 2. SEM morphologies of the cross-section of the oxide scale on the surface of implanted and un-implanted Ferritic Steel oxidized at 900°C

Fig. 2 shows the cross-sectional of oxide scale formed on the implanted and un-implanted ferritic steels oxidized at 900°C. The oxide scale on the surface of an-implanted ferritic steel is formed up to a scale thickness of 600 μm, where the oxide scales show mainly consisted of Cr_2O_3 about 33.47 and FeO 99.40 at%. However, the adherence between scale and a base metal reduced causes the occurrences of the largest crack along the scale. For the specimen that implanted with lanthanum show better oxide scale indicated by the thickness of the oxide scale was found about 300 μm thick, although the cracking also occurs but the presence of Cr_2O_3 as the protective layers is still significant in the range of 34.53-36.83 %. While, the presence of Cr_2O_3 on the oxide scale of FeCr that implanted with titanium was found in the range 10.38-29.43 at %. This phenomenon indicates that the implantation of lanthanum has influenced the formation stable layer of Cr_2O_3 and plasticity as well as protects it from evaporation and cracks on high temperature oxidation. The results of the cross-sectional analysis as described above have been confirmed by the results of the oxidation kinetics of both type specimens oxidized at 900°C as shown by following picture.

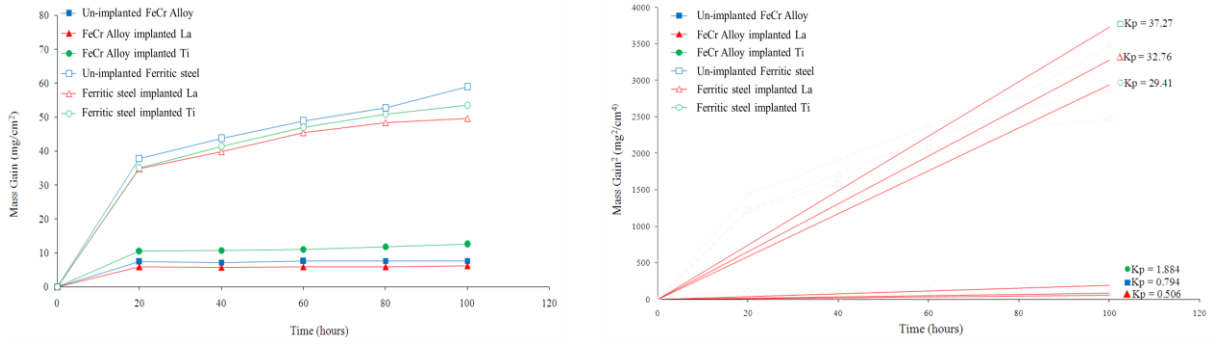

Mass gain curves
a

Parabolic rate curves
b

Figure 3. Mass gain curves and parabolic rate curves of un-implanted and implanted specimens oxidized at 900°C

Figs. 3 show the mass gain curves and parabolic rate curves of the implanted and un-implanted of FeCr alloys and Ferritic steel oxidized at 900°C. Mass gain curves and parabolic rate curves indicates that ferritic steels displayed higher mass gain trend and exhibits poor oxidation resistance. The beneficial effect of lanthanum implantation is clearly visible, the oxidation behaviour being improved. In fact, the mass gain and parabolic rate more lowest, if compared with the un-implanted and Ti implanted specimens. The effect of lanthanum implantation for specimen of FeCr alloy that implanted with lanthanum is significantly to reduce the mass gain change and parabolic rate from 7.73 mg/cm^2 and 0.794 mg^2/cm^4 to 6.29 mg/cm^2 and 0.506 mg^2/cm^4, respectively, in comparing with un-implanted FeCr alloy. Furthermore, The effect of lanthanum implantation for specimen of ferritic steel that implanted with lanthanum is significantly to reduce the mass gain change and parabolic rate from 59 mg/cm^2 and 37.27 mg^2/cm^4 to 49.7 mg/cm^2 and 29.41 mg^2/cm^4, respectively, in comparing with un-implanted ferritic steel. While, the effect of titanium implantation becomes ineffective to reduce the growth of oxide scale which indicates by the highest mass gain change and parabolic rate for both type of specimens. In order to strengthen the analysis result described above, XRD analysis were applied to identified the oxide phase of both type of specimens. The XRD patterns for specimens oxidized at 900°C for100 h are presented in Fig.4.

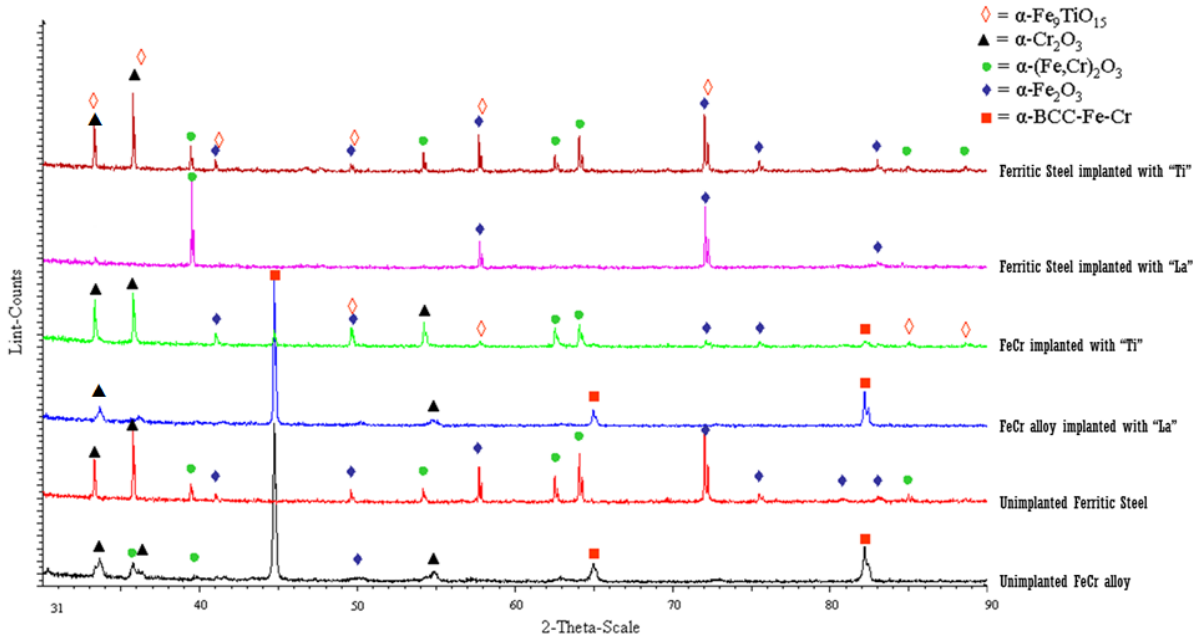

Figure 4. X-rays diffractograms of unimplanted and implanted specimens oxidized for 100 h at 900°C

Fig. 4 above shows the diffraction patterns of FeCr alloys and ferritic steels oxidized at 900°C. For unimplanted FeCr alloy, the signal peaks can be identified as α-$(Fe,Cr)_2O_3$, α-Fe_2O_3, and α-Cr_2O_3. The FeCr phase is also shown, but only on as the developed specimen which indicates the thin of oxide scale on the substrate surface. For the implanted specimens, the main oxide scale obtained were α-$(Fe, Cr)_2O_3$, α-Fe2O3, α-Cr_2O_3. The presence of the peak of the original alloy indicates that oxide scale was formed as a thin layer which dominated by the presence of Cr-rich oxide and small peaks of solid solution chromium iron oxide $(Fe,Cr)_2O_3$ [10, 13-15]. On the contrary, FeCr alloy that implanted with titanium dopant, all strong peaks were dominated by the presence of α-Fe_9TiO_{15}, hematite Fe_2O_3 and small peaks of solid solution chromium iron oxide $(Fe,Cr)_2O_3$, although the presence of the peaks of the original alloys still found with a small intensity which indicates that oxide scale was growing rapidly with the dominating presence of Fe-rich oxide due to ineffectively of titanium implantation. In order to understand more detail about the mechanism of oxide growth on the surface of specimens, EDX line/mapping analysis was used to verify the results in the formation of the oxide scale of FeCr and ferritic steel that implanted with lanthanum as the best oxidation results as shown in Fig.5 and 6.

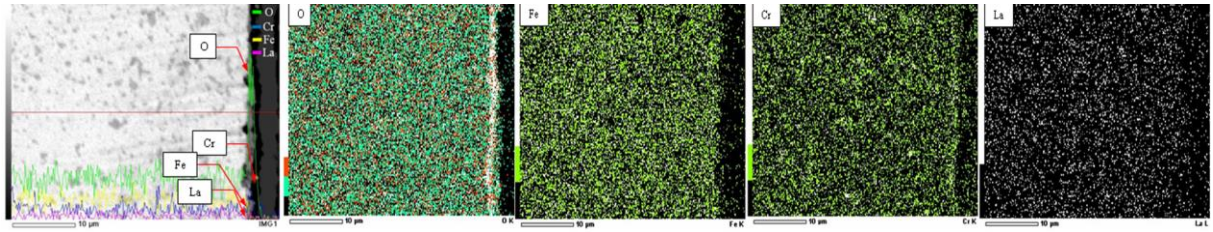

Figure 5. Cross-sectional EDS mapping analysis of FeCr implanted with La oxidized at 900°C

Fig.5 above shows that the scale formed on FeCr alloy that implanted with lanthanum consisted of corundum oxides layer of Cr_2O_3 wich confirmed by EDX mapping analyses which indicated by high presence of Cr rich oxide on the inner of oxide scale, while, the EDX mapping analyses indicates that the presence of Fe was found on the outer of oxide scale with small amount of Fe on the formation of FeO. However, EDX mapping analyses is not clear to detect the presence of Lanthanum on the oxide scale due to low doses of Lanthanum that implanted in to substrate of the alloy. This phenomenon indicates that the lanthanum implantation significantly to reduce the growth of oxide scale by reducing the Cr^{3+} ions diffuses to the surface of the specimens. where the enhancement of Cr diffusion guarantee the stable growth of the Cr-rich in the inner of the oxide scales, which significantly improve oxidation resistance, even a Cr_2O_3 scale may be formed at higher temperatures owing to the higher diffusion rate of Cr.

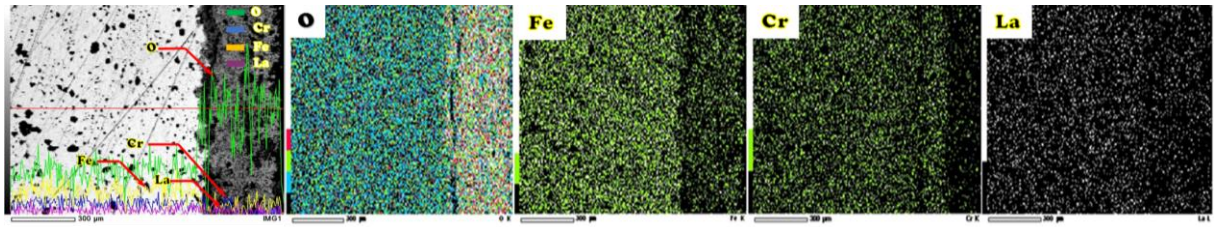

Figure 6. Cross-sectional EDS mapping analysis of ferritic steel implanted with La oxidized at 900°C

Fig.6 above shows that the Cr concentration in ferritic steel is still not sufficiently high to allow the formation of a more protective Cr_2O_3 layer, while the iron ions dissolve in and diffuse rapidly through the Cr_2O_3 scale and eventually an outer layer of fairly pure iron oxides will result. It may be caused by Fe and Cr ion transport is predominant then make the scale growth will proceed outwards, the oxygen transports through the FeO layer to the Cr_2O_3 layer and the Cr ions diffuse to the same layer; both of them react with each other, which make the oxide scale become thicker. Furthermore, due to the loose and incompact scale, thus causing the crack in the surface of the specimen which increase the rate of Cr evaporation. The oxygen may diffuse to the oxidation/alloy interface through the cracks and pores in the oxide scale. This phenomenon was confirmed by XRD results as shown in Fig. 3, where the result shows that the oxide phase that formed on the surface of ferritic steel that implanted with lanthanum is dominated by the presence of Fe_2O_3. It's also reinforcement by mass gain change and parabolic rate constant (k_p) as presented in Fig. 3. It can be noticed that a discontinuous Cr_2O_3 scale was formed, but could not protect the alloy from internal oxidation. At the same time, Fe became enriched and diffused outwards, which caused the formation and rapid growth of FeO, although it has been implanted with lanthanum due to the higher crystallite size effect.

4. Conclusion

Based on the results obtained in the oxidation of implanted and un-implnted FeCr alloys and ferritic steel at 900°C for 100 h the following conclusions can be formulated:

1. The oxidation resistance of FeCr alloy that implanted with Lanthanum showed better quality than that of commercial alloy. The beneficial effect of La implanted sample on the oxidation resistance was clearly visible to improve the adherence of oxide scale. Cross-sectional observations revealed the effectiveness of La implantation for improving thinner and stronger

scale/substrate interface during oxidation process which presents the homogenous structure with good adherence and a uniform inter-diffusion layer between substrate and oxide layer.

2. The specimens that implanted with lanthanum show better promoting the formation of Cr_2O_3 in large amount compositions which indicated that chromium preference diffused outward to form a Cr_2O_3 layer.
3. The oxide scale formed on the surface of FeCr alloys and ferritic steel that implanted with titanium dopant was thicker oxide scales indicating that significant increase in oxidation weight gain. It can be noticed that titanium implantation ineffectively promotes Cr rich oxide. At the same time, the amount of Fe increased and diffused outwards, which caused the formation and rapid growth of FeO. Furthermore, FeO nucleated and grew at the discontinuous areas such as the incompact Cr_2O_3 scale or its micro-defective areas; leading to some bulges and cracks.

5. References

[1] Kulekci, M. K. 2008. Magnesium and its alloys applications in automotive industry. *The International Journal of Advanced Manufacturing Technology*, *39*(9), 851-865.

[2] Cooper, L., Benhaddad, S., Wood, A., & Ivey, D. G. 2008. The effect of surface treatment on the oxidation of ferritic stainless steels used for solid oxide fuel cell interconnects. *Journal of Power Sources*, *184*(1), 220-228.

[3] Korsunsky, A. (Ed.). 2012. *Current Themes in Engineering Science 2010*. American Institute of Physics.

[4] Hui, R. 2013. Materials and Processing for Metal-Supported Solid Oxide Fuel Cells. *Materials for High-Temperature Fuel Cells*, 309-340.

[5] Saryanto, H., Deni, S. K., Untoro, P., Saleh, M. H., & Sebayang, D. 2010. Determination of Nanocrystalline Fe80Cr20 Powder based Alloys using Williamson-Hall Method. In *Advanced materials research* (Vol. 129, pp. 999-1003). Trans Tech Publications.

[6] Sachitanand, R., Sattari, M., Svensson, J. E., & Froitzheim, J. 2013. Evaluation of the oxidation and Cr evaporation properties of selected FeCr alloys used as SOFC interconnects. *international journal of hydrogen energy*, *38*(35), 15328-15334.

[7] Ali-Löytty, H. 2013. Microalloying Mediated Segregation and Interfacial Oxidation of FeCr Alloys for Solid-Oxide Fuel Cell Applications. *Tampereen teknillinen yliopisto. Julkaisu-Tampere University of Technology. Publication; 1114*.

[8] Saryanto, H., Sebayang, D., & Untoro, P.2017, May. Cross-Sectional Investigations of Oxide Scale Nanocrystalline FeCr Alloys after High-Temperature Oxidation Test at 900° C. In *IOP Conference Series: Materials Science and Engineering* (Vol. 196, No. 1, p. 012030). IOP Publishing.

[9] Hilpert, K., Quadakkers, W. J., & Singheiser, L. 2003. Interconnects. *Handbook of Fuel Cells*.

[10] Sebayang, D., Khaerudini, D. S., Saryanto, H., Othman, M. A., Sujitno, T., & Untoro, P. (2011). Effect of Nanocrystalline and Ti implantation on the oxidation behaviour of Fe80Cr20 alloy and commercial ferritic steel. In *Key Engineering Materials* (Vol. 474, pp. 2134-2139). Trans Tech Publications.

[11] Lessing, P. A. 2007. A review of sealing technologies applicable to solid oxide electrolysis cells. *Journal of Materials Science*, *42*(10), 3465-3476.

[12] Akanda, S. R. 2012. *Mechanical Characterization of Coating-Interconnect Interfaces and Anode-Electrolyte Interfaces for Solid Oxide Fuel Cells*. The Ohio State University.

[13] Sebayang D *et al* Oxidation Resistance of $Fe_{80}Cr_{20}$ Alloys Treated by Rare Earth Element Ion Implantation. Current Themes In Engineering Science 2010: *AIP Conference Proceedings*. 1394. No. 1 pp 90-102.

[14] Hendi, S., Darwin, S., Pudji, U, & Tjipto, S. 2009. Ion implantation process of Lanthanum and Titanium Dopants into a substrate of Fe80 Cr20.

[15] Sebayang, D., Khaerudini, D. S., Saryanto, H., Omar, B., Othman, M. A., Hamid, A &

Untoro, P. 2011. Oxidation Resistance of Unimplanted and Implanted of Nanocrystalline FeCr Alloy and Commercial Alloy with Lanthanum. *Journal of Advanced Microscopy Research*, *6*(4), 263-277.